

# Line conditioning system with simple control strategy and fast dynamic response

L. Morán  
E. Mora  
R. Wallace  
J. Dixon

Indexing terms: Line conditioning systems, Power factor compensation, Inverters

**Abstract:** The performance and dynamic characteristics of a solid-state line conditioning system which simultaneously eliminates line current harmonics and compensates load power factor is presented and analysed. The line conditioning system is implemented with a pulsewidth modulated voltage-source inverter. Power factor compensation is achieved by controlling the magnitude and the phase angle ( $\delta$ ) of the transistorised PWM inverter output voltage through a modulation index control. The principal advantage of this scheme is that it can maintain a near unity mains overall power factor without sensing and computing the associated reactive power component. It can also substantially reduce the harmonic content of the line current when the load is nonlinear. A time domain model is derived and used to accurately predict dynamic behaviour, the stability region and to adjust system controllers. The transfer function of the line conditioning system for open-loop and closed-loop operation is derived. Experimental results confirm the operation characteristics obtained by computer simulation and mathematical analyses.

## 1 Introduction

In recent years more stringent requirements have been applied to the performance of reactive power compensators. With the proliferation of harmonic-producing loads, including the increasing number of static power converters, a fast acting line conditioning system will have to be considered as an essential component of an industrial installation. Solid-state active power filters using force-commutated converters are therefore being proposed and are gradually being recognised as a viable

© IEE, 1995

Paper 1485C (P6, P7), first received 28th October 1993 and in revised form 18th July 1994

L. Morán, E. Mora and R. Wallace are with the Department of Electrical Engineering, Universidad de Concepción, Casilla 53-C, Concepción, Chile

J. Dixon is with the Department of Electrical Engineering, Universidad Católica de Chile, Casilla 6177, Santiago, Chile

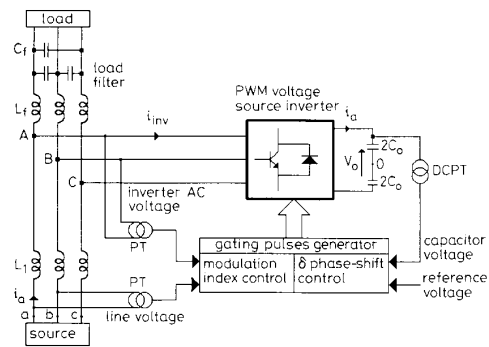


Fig. 1 Line conditioning system configuration

solution to the problems created by static converters and other nonlinear loads [1-4].

The topology of the line conditioning system presented in this paper is shown in Fig. 1. The proposed configuration is based on a force-commutated pulsewidth-modulated voltage-source inverter connected to a DC capacitor. By connecting the synchronous link reactor  $L_1$  (Fig. 1) in series with the power source instead of at the AC terminals of the PWM inverter, the line conditioning system behaviour is improved and the control scheme becomes simpler and cheaper. In this case, the power factor of the AC supply is controlled by forcing the amplitude of the inverter AC output voltage to be slightly higher or equal to the amplitude of the AC supply voltages. This provides a simple control scheme requiring minimum sensing (line and converter voltages only) and no reactive power calculation. Previous works [5-8] have proved that the dynamic response of the synchronous var compensator with phase-shift control is slow and

The authors would like to acknowledge the financial support from the Fondo de Desarrollo Científico y Tecnológico, 'FONDECYT' through the 91-0400 Project. Also the authors would like to thank the 'Dirección de Investigación' of the University of Concepción and the AID for the assistance given through the projects # 20.92.11 and ICA # 416 respectively.

depends on the values of the synchronous link inductor  $L_1$  and the DC capacitor  $C_0$ . To improve the transient response of the line conditioning system presented in this paper, a control circuit composed of a delta phase-shift angle combined with a modulation index control loop is proposed. The delta phase-shift angle control loop keeps the DC voltage constant over the long term by adjusting the small amount of real power absorbed by the inverter [5, 7]. The amplitude of the inverter AC output voltages is controlled by changing the modulation index of the PWM switching pattern. This allows a precise and fast control of the AC mains power factor. Moreover, compared with synchronous solid-state reactive power compensators [1–8], the proposed line conditioning system has the following advantages:

- (a) It does not require reactive current component calculation of the reactive power absorbed by the load.
- (b) It allows continuous power factor control with fast response time (below two cycles of the AC supply).
- (c) It can substantially reduce the amplitude of any line current harmonics generated by nonlinear types of load.

Although a similar line conditioning system configuration was presented and analysed in Reference 5, the compensator proposed in this paper presents better transient compensation characteristics owing to the implementation of a modulation index control loop.

The treatment presented in this paper includes a comprehensive steady-state and transient analysis of the line conditioning system. The stability region and closed-loop control tuning are obtained from the developed time domain model. Finally, all the predicted results are experimentally verified on a 10 kVA laboratory prototype.

## 2 Principles of operation

The principal power circuit component of the line conditioning system, as shown in Fig. 1, is a force-commutated voltage-source inverter connected to a DC capacitor. The main features of the proposed compensator are the simple control system required to keep the AC mains power factor close to one and the ability to eliminate low-frequency load current harmonics.

### 2.1 Power factor correction

The power factor correction is done by forcing the amplitude of the inverter AC output voltage to be slightly higher, lower or equal to the amplitude of the AC mains voltage (Figs. 2 and 3). In the long term, the inverter AC

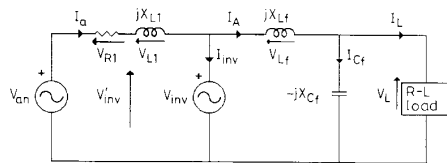


Fig. 2 Single-phase equivalent circuit of the line conditioning system at fundamental frequency

voltage is controlled by adjusting the DC bus voltage through small changes in the amount of real power absorbed by the inverter through a  $\delta$  closed-loop control [5]. Since the time response of the  $\delta$  closed loop is slow

and depends on the value of the synchronous link inductor  $L_1$  and the DC capacitor  $C_0$  [6, 7], the compensator time response is significantly improved with the imple-

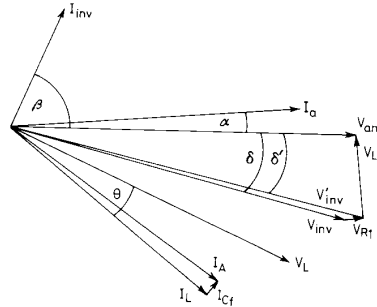


Fig. 3 Generalised phasor diagram for inductive load compensation ( $V_{an} < V_{inv}$ )

mentation of a modulation index control loop. Transiently, the inverter AC output voltage is maintained constant by changing the gating signals modulation index so that the DC voltage variations are compensated.

To be able to continuously change the gating signal modulation index with a simple control circuit, the PWM technique presented in Reference 10 is used. The selected PWM technique allows a maximum voltage gain and low-order harmonic attenuation to be obtained with the lowest possible switching frequency (40% lower than conventional carrier PWM techniques).

Under steady-state operating conditions, the real power absorbed by the inverter is the difference between the real power delivered by the AC source and the real power consumed by the load. The real power provided by the AC source is given by

$$P_{ac} = \frac{V_{an} V_{inv}}{X_1} \sin(\delta) \quad (1)$$

where  $\delta$  is the phase-shift between the source voltage  $V_{an}$  and the fundamental component of the inverter AC voltage  $V_{inv}$ .

Under a load power factor fluctuation, the inverter will transiently supply or absorb the extra real and reactive power delivered by the load, thereby charging or discharging the DC capacitor. To keep the inverter AC output voltage  $V_{inv}$  equal to the amplitude of the corresponding AC mains voltage  $V_{an}$  and the source power factor close to one, the gating signals modulation index changes, and at the same time, the phase-shift angle  $\delta$  is modified so that the inverter will draw or generate more real power from the AC source restoring the DC voltage.

Fig. 4 shows simulated waveforms for fundamental components for a load power factor fluctuation. In particular, Fig. 4a shows the load current  $I_L$  and the respective phase to neutral voltage  $V_{an}$ . Fig. 4b shows the effectiveness of the line conditioning system by keeping the AC mains power factor close to one. Fig. 4c illustrates the DC voltage variation due to the changes in the load power factor and the amplitude of the inverter AC output voltages. It is clear that the modulation index control is able to keep the amplitude of the inverter fundamental output voltage almost constant. Fig. 4d shows the values of the modulation index  $m$  and the phase-shift angle  $\delta$ .

## 2.2 Filtering characteristics

Low-frequency current components generated by nonlinear loads are effectively attenuated by the PWM voltage-

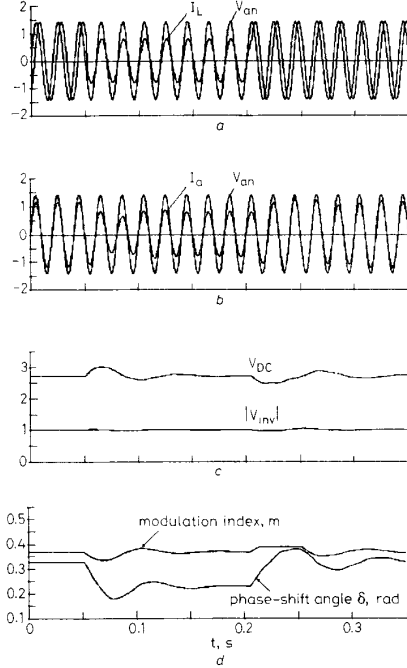


**Fig. 4** Simulated waveforms for linear load compensation and transient operating conditions

a Phase to neutral source voltage  $V_{an}$  and respective load current  $I_L$   
b Source voltage  $V_{an}$  and line current  $I_a$   
c DC voltage fluctuation  $V_{DC}$  and amplitude of the inverter output voltage  $|V_{inv}|$   
d Modulation index value  $m$  (on a phase to neutral bases) and  $\delta$  phase-shift angle

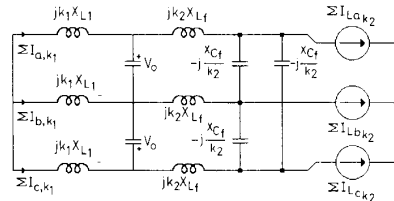


**Fig. 5** Three-phase equivalent circuit for harmonic components of the line conditioning system connected to a nonlinear load

source inverter. The small second-order filter connected between the inverter and the load (Fig. 1) contributes to eliminate high-frequency load current harmonics but is not responsible for the attenuation of low-frequency load current components. Its function is to minimise high-frequency current and voltage harmonics generated by the inverter. Low-frequency current components generated by the load circulate mainly through the voltage-source inverter since it offers a low impedance path. The inverter connects the charged DC capacitor between the

AC lines creating a second-order filter with the respective synchronous link inductor  $L_1$ . Fig. 5 shows the compensator equivalent circuit for the harmonic component at a given instant. Since in the voltage-source inverter three switches are always conducting, the DC capacitor gets reflected to the AC side in an open delta connection. It must be noted that the DC capacitor connection is changed at a rate equal to the inverter switching frequency.

## 3 Time domain model

The time domain model of the line conditioning system is derived considering the single-phase equivalent circuit shown in Fig. 2 and based on the following assumptions:

(a) The three AC source voltages are balanced and contain no harmonics.

(b) The equivalent circuit shown in Fig. 2 only takes into account the fundamental components of current and voltages. The harmonics generated by the PWM voltage-source inverter are neglected. They do not affect the time domain model when they are small enough, as is the case for most of the practical PWM converters.

(c) All the losses of the AC system are lumped and represented by an equivalent resistance  $R_1$  connected in series with the link inductor  $L_1$ .

(d) Switching losses and the power dissipated in the DC capacitor are represented by an equivalent resistance  $R_c$  connected in parallel with the DC capacitor.

It should be noted that the inclusion of a modulation index control loop and the connection of the synchronous link inductor  $L_1$  in series with the power source instead of at the inverter AC terminals changes the mathematical model of the compensator, as compared with the analysis presented in Reference 6. Applying the Kirchhoff voltage law in the equivalent circuit shown in Fig. 2, and then considering a three-phase balanced circuit, the following system equation is obtained:

$$[V] = L_1 \frac{d[i_a]}{dt} + R_1 [i_a] + [V_{inv}] \quad (2)$$

where

$$[V] = \begin{pmatrix} V_{an} \\ V_{bn} \\ V_{cn} \end{pmatrix} = \begin{pmatrix} \sqrt{2}V \sin(\omega t) \\ \sqrt{2}V \sin(\omega t - 120^\circ) \\ \sqrt{2}V \sin(\omega t + 120^\circ) \end{pmatrix}$$

$$[V_{inv}] = \begin{pmatrix} V_{inva} \\ V_{invb} \\ V_{invc} \end{pmatrix} = \begin{pmatrix} \sqrt{2}V_{inv} \sin(\omega t - \delta) \\ \sqrt{2}V_{inv} \sin(\omega t - 120^\circ - \delta) \\ \sqrt{2}V_{inv} \sin(\omega t + 120^\circ - \delta) \end{pmatrix} \quad (3)$$

$m$  is the inverter modulation index, defined as

$$m = \frac{V_{inv}}{V_{DC}} \quad (4)$$

where  $V_{inv}$  is the fundamental component RMS value of the inverter phase to neutral voltage and  $V_{DC}$  is the voltage across the DC capacitor.

The dynamic model of the power factor compensator given in eqn. 2 may be transformed into a time invariant dynamic model by an  $abc$ - $dqo$  transformation of reference frame. That is

$$[V]_{dqo} = [R_1]_{dqo} [i_a]_{dqo} + [L_1]_{dqo} \frac{d[i_a]_{dqo}}{dt} + [A][L_1] \frac{d[A]}{dt} [i_a]_{dqo} + [V_{inv}]_{dqo} \quad (5)$$

where

$[R_1]_{dqo} = [A][R_1][A]^t$  and  $[L_1]_{dqo} = [A][L_1][A]^t$  and  $[A]$  is the  $abc$ - $dqo$  transformation matrix,  $[V]_{dqo}$  and  $[V_{inv}]_{dqo}$  are the source and inverter output voltages in the  $dqo$  frame.

$$[A] = \sqrt{\frac{2}{3}} \begin{pmatrix} \cos \omega t & \sin \omega t & 1/\sqrt{2} \\ \cos(\omega t - 120^\circ) & \sin(\omega t - 120^\circ) & 1/\sqrt{2} \\ \cos(\omega t + 120^\circ) & \sin(\omega t + 120^\circ) & 1/\sqrt{2} \end{pmatrix} \quad (6)$$

and

$$[V]_{dqo} = [A]^t [V]_{abc} = \begin{pmatrix} 0 \\ \sqrt{3}V \\ 0 \end{pmatrix}$$

$$[V_{inv}]_{dqo} = [A]^t [V_{inv}]_{abc} = \begin{pmatrix} -\sqrt{3}V_{inv} \sin(\delta) \\ \sqrt{3}V_{inv} \cos(\delta) \\ 0 \end{pmatrix} \quad (7)$$

Replacing eqns. 6 and 7 in eqn. 5 and developing

$$L_1 \frac{di_{ad}}{dt} = -R_1 i_{ad} - \omega L_1 i_{aq} + \sqrt{3}V_{inv} \sin(\delta) \quad (8)$$

$$L_1 \frac{di_{aq}}{dt} = -R_1 i_{aq} + \omega L_1 i_{ad} + \sqrt{3}V - \sqrt{3}V_{inv} \cos(\delta) \quad (9)$$

Eqns. 8 and 9 represent the time-invariant dynamic model of the line conditioning system. The power absorbed by the inverter in the  $dqo$  frame is given by

$$P_{inv} = i_{invd} V_{invd} + i_{invq} V_{invq} \quad (10)$$

The power balance equation in the  $dqo$  frame is equal to

$$\frac{V_{DC}^2}{R_c} + C V_{DC} \frac{dV_{DC}}{dt} = (i_{invd} V_{invd} + i_{invq} V_{invq}) \quad (11)$$

The left term in eqn. 11 represents the losses in the DC capacitor and in the inverter switches and the instantaneous power stored in the DC capacitor. Applying the current Kirchhoff law at the inverter terminals, the following equations are obtained:

$$i_{invd} = i_{ad} - i_{Ad}$$

$$i_{invq} = i_{aq} - i_{Aq} \quad (12)$$

Finally, by replacing eqns. 12 and 7 in eqn. 11 the power balance equation of the inverter becomes

$$C \frac{dV_{DC}}{dt} = \sqrt{3}m\{(i_{aq} - i_{Aq}) \cos(\delta) - (i_{ad} - i_{Ad}) \sin(\delta)\} - \frac{V_{DC}}{R_c} \quad (13)$$

The equations that describe the system behaviour in open-loop operating conditions are eqns. 4, 8, 9 and 13. The unknown variables are  $V_{DC}$ ,  $i_{aq}$  and  $i_{ad}$ . The closed-loop model of the line conditioning system is obtained by including the equations of the PI controllers for the  $\delta$  and the modulation index loops. These equations are

$$\delta(t) = K_{pv} e_v + K_{iv} \int_0^t e_v dt \quad (14)$$

and

$$m(t) = K_{pm} e_m + K_{im} \int_0^t e_m dt \quad (15)$$

where  $\delta(t)$  is the instantaneous value of the phase-shift angle,  $m(t)$  is the instantaneous value of the inverter modulation index,  $K_{pv}$  is the proportional gain of the  $\delta$  loop,  $K_{iv}$  is the integral gain of the  $\delta$  loop,  $e_v$  is the error voltage =  $V_{dref} - V_{DC}$ ,  $K_{pm}$  is the proportional gain of the modulation index loop,  $K_{im}$  is the integral gain of the modulation index loop and  $e_m$  is the inverter output voltage error =  $V - V_{ao1}$ .

By solving eqns. 4, 8, 9, 13, 14 and 15 for different load power factor values (defined by  $i_{Ad}$ ), the dynamic performance of the line conditioning system is accurately simulated. The influence of the PI controllers in the compensator time response and the influence of the power circuit components in the line conditioning system response may be obtained by simulation.

Fig. 6 shows that the DC capacitor value plays a significant role in the line conditioning system response

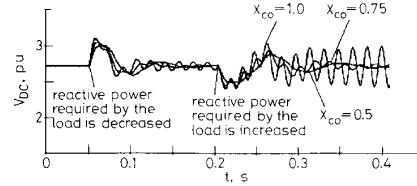


Fig. 6 Simulated capacitor voltage for different capacitance values and for a step change in the reactive power value required by the load

since it is the power component that has to absorb or deliver the instantaneous power generated or absorbed by the load. Smaller values of  $C$  generate an oscillating DC voltage responses whereas larger values of  $C$  make  $V_{DC}$  more stable.

Also, simulated results show that system stability is improved if the two control loops are decoupled by forcing the  $\delta$  loop to be at least 10 times slower than the modulation index control loop. Also, these results prove that the compensator stability increases if the  $X_1/R_1$  ratio is below 15 since  $R_1$  provides the damping required by  $i_{ad}$  and  $i_{aq}$ .

#### 4 Transfer function of the line conditioning system

The mathematical model derived in the previous Section shows that the line conditioning system is a multivariable nonlinear system. To obtain its transfer function the system eqns. 8, 9 and 13 must be linearised, applying small perturbations around an operating point. This method is valid since in practice the variations of the phase-shift angle  $\Delta\delta$  and the modulation index  $\Delta m$  are small.

Considering eqn. 8

$$\frac{di_{ad}}{d(\omega_0 t)} = \frac{-R_1}{X_1} i_{ad} - i_{aq} + \frac{\sqrt{3}}{X_1} V_{inv} \sin(\delta) \quad (16)$$

applying small perturbations around the operating point in eqn. 16 and then subtracting the steady state equation

$$\frac{\Delta i_{ad}}{d(\omega_0 t)} = \frac{-R_1}{X_1} \Delta i_{ad} - \Delta i_{aq} + \frac{\sqrt{(3)}}{X_1} \delta_0 \Delta V_{inv} + \frac{\sqrt{(3)}}{X_1} V_{inv_0} \Delta \delta \quad (17)$$

where the subscript 'o' denotes steady-state value. Applying the Laplace transform in eqn. 17.

$$s \Delta i_{ad} = \frac{-R_1}{X_1} \Delta i_{ad} - \Delta i_{aq} + \frac{\sqrt{(3)}}{X_1} \delta_0 \Delta V_{inv} + \frac{\sqrt{(3)}}{X_1} V_{inv_0} \Delta \delta \quad (18)$$

where  $s = \omega/\omega_0$ . Doing the same analysis for eqn. 9 gives

$$s \Delta i_{aq} = \frac{-R_1}{X_1} \Delta i_{aq} + \Delta i_{ad} - \frac{\sqrt{(3)}}{X_1} \Delta V_{inv} \quad (19)$$

Solving eqns. 18 and 19 for  $\Delta i_{ad}$  and  $\Delta i_{aq}$

$$\Delta i_{ad} = \frac{\frac{\sqrt{(3)}}{X_1} \left\{ \left( \delta_0 s + \delta_0 \frac{R_1}{X_1} + 1 \right) \Delta V_{inv} + \left( V_{inv_0} s + V_{inv_0} \frac{R_1}{X_1} \right) \Delta \delta \right\}}{s^2 + 2 \frac{R_1}{X_1} s + 1 + \left( \frac{R_1}{X_1} \right)^2} \quad (20)$$

$$\Delta i_{aq} = \frac{\frac{\sqrt{(3)}}{X_1} \left\{ \left( \delta_0 - \left( s + \frac{R_1}{X_1} \right) \right) \Delta V_{inv} + V_{inv_0} \Delta \delta \right\}}{s^2 + 2 \frac{R_1}{X_1} s + 1 + \left( \frac{R_1}{X_1} \right)^2} \quad (21)$$

The power balance equation of the power factor compensator may be represented by the normalised equation

$$\frac{dV_{DC}}{d(\omega_0 t)} + \frac{X_c}{R_c} V_{DC} = \sqrt{(3)} m X_c (i_{invq} - \delta i_{invd}) \quad (22)$$

$X_c = 1/\omega C$ , the DC capacitor reactance at the AC mains frequency. Since  $\delta$  is small,  $\cos \delta = 1$  and  $\sin \delta = \delta$ . Applying small perturbations around the steady-state operating point gives

$$\begin{aligned} m i_{invq} &= m_0 i_{invq_0} + i_{invq_0} \Delta m + m_0 \Delta i_{invq} \\ m \delta i_{invd} &= m_0 \delta_0 i_{invd_0} + \delta_0 i_{invd_0} \Delta m \\ &\quad + m_0 i_{invd_0} \Delta \delta + m_0 \delta_0 \Delta i_{invd} \end{aligned} \quad (23)$$

Replacing eqns. 23 in eqn. 22, neglecting second-order terms and subtracting the steady state equation gives

$$\begin{aligned} \frac{d\Delta V_{DC}}{d(\omega_0 t)} + \frac{X_c}{R_c} \Delta V_{DC} &= \sqrt{(3)} X_c \{ (i_{invq_0} - \delta_0 i_{invd_0}) \Delta m \\ &\quad + m_0 \Delta i_{invq} - m_0 \delta_0 \Delta i_{invd} - m_0 i_{invd_0} \Delta \delta \} \end{aligned} \quad (24)$$

Applying the Laplace transform

$$\begin{aligned} \left( s + \frac{X_c}{R_c} \right) \Delta V_{DC} &= \sqrt{(3)} X_c \{ (i_{invq_0} - \delta_0 i_{invd_0}) \Delta m \\ &\quad + m_0 \Delta i_{invq} - m_0 \delta_0 \Delta i_{invd} - m_0 i_{invd_0} \Delta \delta \} \end{aligned} \quad (25)$$

The transfer function of the line conditioning system is obtained by replacing  $\Delta i_{invd}$  by  $\Delta i_{ad} - \Delta i_{ad}$  and  $\Delta i_{invq}$  by  $\Delta i_{aq} - \Delta i_{aq}$  and then replacing  $\Delta i_{ad}$  and  $\Delta i_{aq}$  by eqns. 20 and 21. To simplify the mathematical model,  $\Delta i_{aq}$  is neglected since the changes in the reactive component required by the load depends mainly on  $\Delta i_{ad}$  (Fig. 6).

$$\begin{aligned} \Delta V_{DC} &= G_1(s) \Delta m + G_2(s) \Delta V_{inv} \\ &\quad + G_3(s) \Delta \delta + G_4(s) \Delta i_{2d} \end{aligned} \quad (26)$$

where the transfer functions  $G_1(s)$ ,  $G_2(s)$ ,  $G_3(s)$  and  $G_4(s)$  are equal to

$$G_1(s) = \frac{\sqrt{(3)} X_c (i_{invq_0} - \delta_0 i_{invd_0})}{s + \frac{X_c}{R_c}} \quad (27)$$

$$G_2(s) = \frac{-3m_0(\delta_0^2 + 1) \frac{X_c}{X_1} \left( s + \frac{R_1}{X_1} \right)}{\left( s + \frac{X_c}{R_c} \right) \left( s^2 + \frac{2R_1}{X_1} s + \left( \frac{R_1}{X_1} \right)^2 + 1 \right)} \quad (28)$$

$$G_3(s) = \frac{-\sqrt{(3)} m_0 X_c i_{invd_0} \{ \Gamma(s) \}}{\left( s + \frac{X_c}{R_c} \right) \left( s^2 + \frac{2R_1}{X_1} s + \left( \frac{R_1}{X_1} \right)^2 + 1 \right)} \quad (29)$$

and

$$\begin{aligned} \Gamma(s) &= s^2 + \left( \frac{\sqrt{(3)} \delta_0 V_{inv_0}}{X_1 i_{invd_0}} + \frac{2R_1}{X_1} \right) s \\ &\quad + \frac{\sqrt{(3)}}{i_{invd_0} X_1} \left( \frac{\delta_0 R_1}{X_1} - V_{inv_0} \right) + 1 + \left( \frac{R_1}{X_1} \right)^2 \end{aligned} \quad (30)$$

$$G_4(s) = \frac{\sqrt{(3)} m_0 \delta_0 X_c}{\left( s + \frac{X_c}{R_c} \right)} \quad (31)$$

Eqn. 26 shows the line conditioning system transfer function considering  $\Delta V_{DC}$  (fluctuation in the DC capacitor)

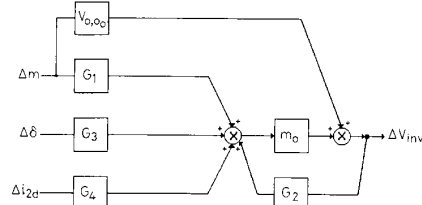


Fig. 7 Open-loop block diagram of the line conditioning system

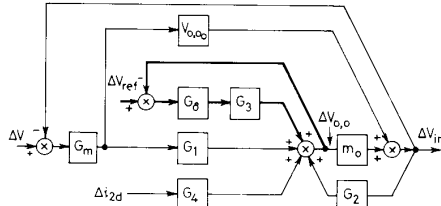
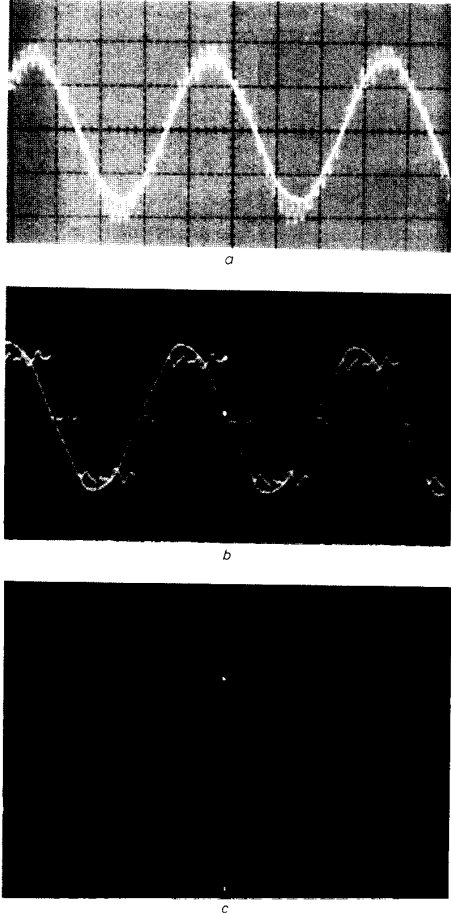


Fig. 8 Closed-loop block diagram of the line conditioning system

as an output. To obtain the inverter AC output voltage as the compensator output variable, the following equation must be considered:

$$\Delta V_{inv} = m_0 \Delta V_{DC} + V_{DC} \Delta m \quad (32)$$



**Fig. 9** Steady state results for nonlinear compensation  
*a* Phase to neutral voltage  $V_m$  (50 V/div) and respective line current (2 A/div)  
*b* Phase to neutral voltage  $V_m$  and respective load current (2 A/div)  
*c* Inverter AC current (5 A/div) and inverter voltage (50 V/div)

The open-loop and the closed-loop block diagram of the proposed line conditioning system are shown in Figs. 7 and 8.

In Fig. 8  $G_m$  and  $G_\delta$  are the transfer function of the PI controllers of the modulation index and the delta loop, respectively. From the analysis of the open-loop system transfer function the following conclusions are obtained:

(a) The solution of the transfer functions characteristics eqns. 27, 28, 29 and 31 proves that the line conditioning system is stable for open-loop operating conditions.

(b) Also, the poles of the line conditioning system show that the open-loop transient response of the compensator

depends mainly on the ratio between  $R_1$  and  $X_1$  (synchronous link reactor) and between  $R_c$  and  $X_c$ .

(c) The negative feedback of  $G_2(s)$ , Fig. 7, defines the open-loop self regulated characteristics of the proposed line conditioning system.

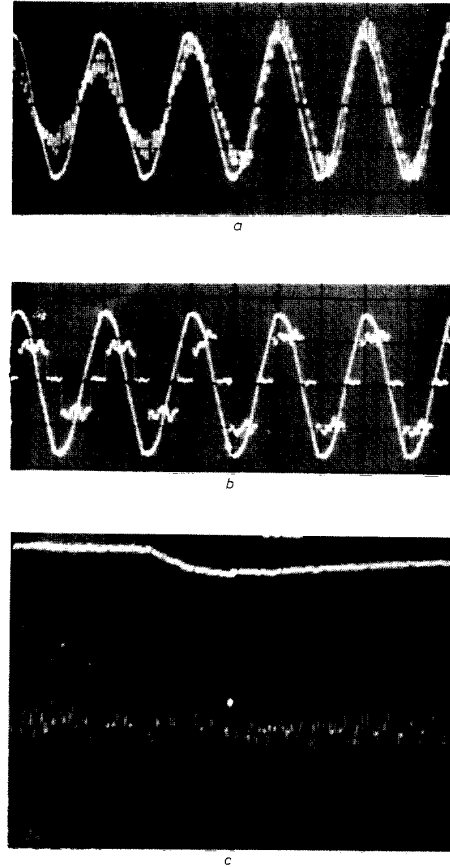


**Fig. 10** Transient experimental results  
*a* Phase to neutral voltage (50 V/div) and respective line current (2 A/div, 10 ms/div)  
*b* Phase to neutral voltage (50 V/div) and respective load current (2 A/div, 10 ms/div)  
*c* DC voltage and DC current (20 ms/div)

The delta phase-shift angle closed loop relates  $\Delta V_{DC}$  with  $\Delta V_{ref}$ , while the modulation index closed loop relates  $\Delta V_{inv}$  with  $\Delta V_{DC}$ . The transfer function of the PI controllers used in both closed loops are  $G_\delta$  and  $G_m$ , respectively.

## 5 Experimental results

To demonstrate the feasibility of the proposed line conditioning system and the associated control schemes an experimental 10 kVA unit was implemented. Steady-state results obtained with this bread board unit are depicted in Figs. 9 and 10.

Steady-state experimental results for a nonlinear compensation are illustrated in Fig. 9. Fig. 9a shows the phase to neutral source voltage and the respective line current. It is evident that the line power factor is one. Fig. 9b depicts the load current (three-phase controlled rectifier) and the respective phase to neutral source voltage  $V_{an}$ . Finally, Fig. 9c shows the inverter AC current and the respective line to line inverter voltage.

Transients results are shown in Fig. 10. The transient operating condition is obtained by generating a step change in the load power factor value. The load power factor value is changed by modifying the firing angle (from  $\alpha = 120^\circ$  to  $\alpha = 60^\circ$ ) of the three-phase controlled rectifier used as a load. In particular Fig. 10a shows the line current and the respective phase to neutral voltage. This Figure proves that the compensator time response is close to three cycles. Fig. 10b depicts the change in the load power factor. Finally, Fig. 10c shows how the DC voltage changes when the load power factor is modified. It is important to note that the time required by the capacitor to reach a steady state is larger than the compensator response. This proves the effectiveness of the modulation index control loop.

Comparison with simulated waveforms shown in Fig. 4 reveals close agreement between predicted and experimental waveforms. Moreover, agreement in waveforms validates the derived model and the analysis presented.

## 6 Conclusions

In this paper a three-phase line conditioning system implemented with a PWM voltage-source inverter that presents a fast response time has been presented and analysed. The proposed line conditioning system can maintain a near unity mains power factor without sensing and computing the associated reactive power

component and it can also substantially reduce low-frequency current harmonics generated by nonlinear types of load. Time response has been improved by including a second closed-loop control that varies the modulation index of the inverter gating signals. The close agreement between the analytical and the experimental results proves the validity of the analysis and the feasibility of the proposed system.

## 7 References

- 1 SUME, Y., *et al.*: 'New static var control using force-commutated inverters', *IEEE Trans.*, 1981, **PAS-100**, (9), pp. 4216-4223
- 2 EDWARDS, C.W., *et al.*: 'Advanced static var generator employing GTO thyristors', *IEEE Trans. on Power Delivery*, 1988, **3**, (4), pp. 1622-1627
- 3 KOJORI, H.A., DEWAN, S.B., and LAVERS, J.D.: 'A large scale PWM solid-state synchronous condenser'. Conf. Record of IEEE Annual Meeting of Ind. Appl., 1990, pp. 1099-1106
- 4 GYUGYI, L.: 'Reactive power generation and control by thyristor circuits', *IEEE Trans.*, 1979, **IA-15**, (5), pp. 521-532
- 5 MORÁN, L., ZIOGAS, P.D., and JOOS, G.: 'Analysis and design of a novel three-phase solid-state power factor compensator and harmonic suppressor system', *IEEE Trans.*, 1989, **IA-25**, (4), pp. 400-407
- 6 JOOS, G., MORÁN, L., and ZIOGAS, P.D.: 'Performance analysis of a PWM inverter var compensator', *IEEE Trans. on Power Electronics*, 1991, **6**, (3), pp. 380-391
- 7 DIXON, J.W., and VEAS, D.: 'Stability analysis and performance characteristics of open loop var compensator'. Conf. Record of IEEE Annual Meeting of Ind. Appl., 1990, pp. 1086-1091
- 8 KOJORI, H.A., LAVERS, J.D., and DEWAN, S.B.: 'A critical assessment of the continuous-system approximate method for the stability analysis of a sampled data system'. Conf. Record of IEEE PESC, 1990, pp. 80-87
- 9 MORÁN, L., ZIOGAS, P.D., and JOOS, G.: 'Analysis and design of a synchronous solid-state var compensator', *IEEE Trans.*, 1989, **IA-25**, (4), pp. 598-608
- 10 ZIOGAS, P.D., MORÁN, L., JOOS, G., and VINCENTI, D.: 'A refined PWM scheme for voltage and current source converters'. Conf. Record of IEEE Annual Meeting of Ind. Appl., 1990, pp. 977-983